Emission of low-energy electrons from slow N^{6+} ions interacting with a Au surface

D. Niemann, M. Grether, A. Spieler, and N. Stolterfoht
Hahn-Meitner-Institut, Bereich FD, Glienicker Strasse 100, 14109 Berlin, Germany

C. Lemell, F. Aumayr, and H. P. Winter
Institut für Allgemeine Physik, Technische Universität Wien, 1040 Wien, Austria

(Received 2 April 1997)

Low-energy electrons emitted during the interaction of N^{6+} ions with a Au surface were measured. The projectile energy was varied in a wide range from 90 eV to 60 keV. A single-stage spectrometer was used to achieve reliable electron measurements at energies as low as a few eV. The experimental data are compared with simulations based on the classical over-the-barrier model. For slow projectiles the observed low-energy electrons are attributed to autoionizing transitions in high Rydberg states of the projectile. The autoionization electrons provide a signature for the first deexcitation steps of hollow atoms formed above the surface. [S1050-2947(97)03211-3]

PACS number(s): 79.20.Rf, 34.50.Dy, 79.90.+b

I. INTRODUCTION

In the past few years the interaction of highly charged ions with surfaces has received increasing attention by several groups [1–12]. This interest has been generated primarily by the phenomenon of hollow atoms that are produced when highly charged ions approach the surface. The highly charged ion strongly attracts electrons that are captured into high Rydberg states. Hence a hollow atom is created with several electrons in higher orbitals whereas inner shells remain empty. The formation of the hollow atom involves a series of complex processes. These processes have been the subject of intensive research of several groups, who developed a commonly accepted scenario.

At a metal surface the highly charged ion induces an image charge that accelerates the ion towards the solid until the ion is neutralized [13–15]. The image charge also produces a shift of the energy levels in the ion and, moreover, the potential barrier is reduced as the ion approaches the surface [16,17]. At a critical distance, where the height of the potential barrier is smaller than the upper limit of the valence band, electrons from the conduction band of the target are transferred into high Rydberg states of the ion by resonant capture processes. Here the ion is readily neutralized and a hollow atom is formed in front of the surface. When the projectile further approaches the surfaces, lower levels become occupied by resonant capture processes and the energy levels are further shifted by screening effects. Hence the outermost electrons of the hollow atoms may be transferred back into the solid by resonant ionization, i.e., the reverse process of resonant capture. In addition, the electrons may be transferred into the continuum giving rise to free electrons.

Apart from these monoelectronic charge-transfer processes, the above-surface hollow atoms undergo dielectronic processes. For instance, mutual interactions between weakly bound electrons in high Rydberg states give rise to autoionization, where an electron is transferred to a lower level and another electron is emitted. The dielectronic processes play the dominant role in the model by Arifov *et al.* [2], who assumed a total relaxation of the hollow atom in front of the surface due to autoionization processes. However, the interaction time available in front of the surface is limited. The image charge acceleration sets a lower limit to the perpendicular velocity, i.e., an upper limit to the interaction time. Even for very slow projectiles, the Auger rates are too low to allow for the relaxation to the ground state in front of the surface. When the projectile finally enters the increasing electron density of the surface, it is still hollow involving weakly bound electrons [6,18]. These electrons are ''peeled off'' and transferred into the solid or the continuum.

The peel-off process again produces a highly charged ion that attracts several electrons from the conduction band during the passage into the solid. Thus a dynamic screening cloud of quasilocalized electrons is created. This cloud leaves an empty space around the projectile nucleus forming a hollow atom of a relatively small size [19,20]. When the hollow atom further moves within the solid, empty inner orbitals are successively filled by Auger transitions and collisional charge transfer. The Auger electrons travel through the solid where they suffer elastic and inelastic scattering processes. The same is true for conduction-band electrons that received kinetic energy in binary collisions with the projectile. The fast electrons produce an avalanche of secondary electrons, which may overcome the work function and hence leave the surface. These secondary electrons contribute to the low-energy part of the electron spectrum [21].

In the field of electron spectroscopy, most information about the properties of hollow atoms have been obtained by studying K Auger electron emission [22–24]. It should be realized, however, that the K Auger transitions constitute the final step of the filling cascade of the hollow atoms that have usually entered the solid at that instant [25]. To obtain direct information about the hollow atom formation above the surface it is favorable to measure low-energy electrons. When the interaction time is sufficiently long, autoionization transitions occur between highly lying states of the hollow atom giving rise to electrons of a few eV. The low-energy electrons are expected to provide direct information about an early stage of the decaying hollow atom, especially in front of the surface.

 © 1997 The American Physical Society

In the past, low-energy electron emission by highly charged ions at surfaces has been studied extensively using the method of measuring electron-number distributions and the total yields of the ejected electrons [10,26–29]. Regarding the velocity dependence of the total yield, two regions become conspicuous: The total yield of the low-velocity part mainly due to potential-energy emission is essentially constant, whereas the total yield of the high-velocity regime predominantly due to kinetic-energy emission increases with increasing velocity. It is noted, however, that the total electron yield is composed of various contributions for electron emission.

Information about the individual contributions can be obtained from spectroscopic measurements where the energy of the ejected electron is determined [1]. Unfortunately, due to the well-known problems of measuring low-energy electrons, spectroscopy measurements and their detailed analysis are still limited in the field of highly charged ion impact. A few measurements on the electron-emission spectra due to the interaction of highly charged ions with surfaces exist [1,3,30,31]. To our knowledge, no attempt has been made to analyze electron energy spectra with respect to the low-energy autoionization electrons predicted by Arifov *et al.* [2]. In particular, no data are available for slow projectiles with energies as low as 100 eV.

In this work we started measurements where particular effort was devoted to reliable data for electrons at energies of a few eV. We report on double differential emission yields of N^{6+} impact on a monocrystalline clean Au target measured in a wide range of projectile energies. To study the early deexcitation steps of the hollow atom the experimental results are compared with Monte Carlo calculations referring to the fraction of autoionization electrons ejected above the surface. This comparison provides evidence that autoionization electrons ejected above the surface represent an important contribution for projectiles incident at the lowest possible velocity.

II. EXPERIMENTAL METHOD AND DATA ANALYSIS

The experiments were carried out at the 14.5-GHz electron cyclotron resonance source at the Ionenstrahl-Labor of the Hahn-Meitner-Institut, Berlin. The ion source provides particles with energies up to $20q$ keV, where q stands for the charge state of the ion. In front of the experimental setup, i.e., at the end of the beam line, a deceleration lens system is installed to reduce the projectile energies to values as low as $5q$ eV. During the deceleration mode the beam line is set on high voltage and the experimental setup is operated on ground potential.

The experiments were performed in an ultrahigh vacuum chamber, which has been described in detail previously [8]. After accelerating hydrogenlike N^{6+} to $10q$ keV, the ions were analyzed magnetically, decelerated to lower energies, and collimated to a beam spot with a diameter of about 1 mm at the position of the target. The beam diameter was determined by measuring the ion current on a thin wire shifted over the area of the target position.

The experimental setup includes facilities for surface preparation and examination. The base pressure in the chamber was a few 10^{-10} mbar. After carefully cleaning the surface by sputtering and heating no contamination was observed on the surface. The cleanness of the surface was verified by means of electron-induced target Auger electron spectroscopy.

The interaction of the N^{6+} ions with the monocrystalline clean Au target causes the emission of electrons, which were measured with an electrostatic parallel-plate spectrometer [32]. The electron observation angle α relative to the surface can be varied in a wide range. This spectrometer has been used formerly for gas target experiments and was improved in order to fulfill ultrahigh vacuum requirements. Instead of an open photomultiplier previously applied for the detection of the electrons, a channeltron was used.

The spectrometer was optimized for measuring low-energy electrons. It is of a simple design with relatively large slits so that the spectrometer efficiency is rather insensitive to spurious deflections of the electron trajectories. In the spectrometer region the magnetic field was reduced to a few milligauss by a μ-metal shield of the size of the scattering chamber. The spectrometer surface ''seen'' by the electrons was carefully cleaned to avoid disturbing electric fields due to charge-up effects. In order to determine the applicability of the spectrometer with regard to the lowest energy we performed atomic collision experiments of 60 keV O^{6+} with He atoms [33]. The gas target experiments showed that the spectrometer works reliably at electron energies as low as 2 eV.

The spectrometer can be operated either in the normal mode, where one plate is put on the ground potential, or in the high-resolution mode, where the electrons are decelerated to a fixed pass energy. This was achieved by a negative voltage put on the deceleration grids in front of the spectrometer and on the lower deflection plate. In the normal mode the relative resolution is $\Delta E/E = 5.2\%$, whereas the absolute resolution ΔE is constant in the high-resolution mode.

In this work absolute values for electron emission yields were measured. These measurements require the determination of the spectrometer efficiency and the current of the ion beam. The efficiency of the spectrometer was verified from a reaction with a known cross section. For this purpose we measured the emission of Coster-Kronig electrons in collision of 60-keV O^{6+} with He atoms. The cross section for the production of Coster-Kronig electrons was measured to be $(2.8 \pm 0.7) \times 10^{-17}$ cm^2 [33], in good agreement with the previously measured value of 3.3×10^{-17} cm^2 [34]. The number of ions incident on the target was monitored by means of a nanoamperemeter. This relative signal was calibrated on an absolute scale by auxiliary experiments where the incident ion beam was measured in a Faraday cup located behind the target. For this measurement the target holder was temporarily lifted from the beam area.

Figure 1 shows experimental results of double differential emission yields as a function of the electron energy for an angle of incidence of $\psi = 90°$ and an observation angle of $\alpha = 40°$ relative to the target surface. Data are shown for four different projectile energies of 90 eV, 270 eV, 3 keV, and 60 keV, measured in the low-resolution mode of the spectrometer. The errors for the absolute yields are caused by different effects. The main sources of error originate from the determinations of the spectrometer efficiency and the ion current incident on the target. The different errors sum up to

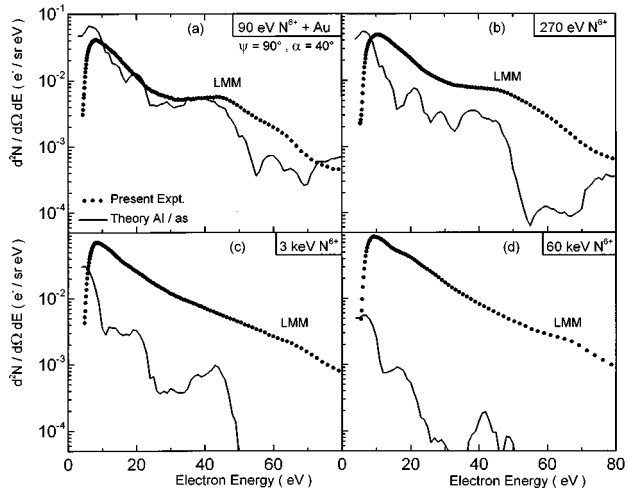

FIG. 1. Comparison of measured double differential cross sections (dots) with model calculations (line) for N^{6+} incident on a Au surface for four different projectile energies. The simulation concerns merely the emitted electrons due to autoionization above the surface (AI/as).

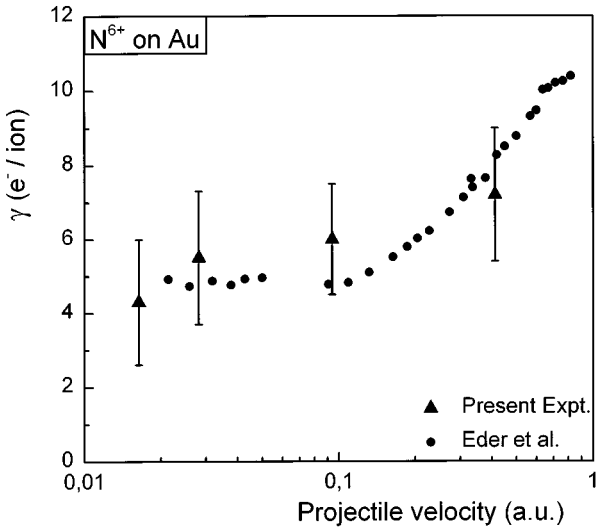

FIG. 2. Measured total electron yields (triangles) and published data from Eder *et al.* [29] versus projectile velocity.

an uncertainty of about $\pm 25\%$ for projectile energies larger than about 1 keV. For slow projectiles the current measurements were uncertain as the collimation of the ion beam was difficult due to low intensity and enhanced beam divergence. At 90 eV the error of the absolute values is as large as $\pm 40\%$.

The low-energy part (<10 eV) of the spectrum is affected by additional errors, which are difficult to estimate. Usually, they are produced by charge-up effects of the target giving rise to small electrostatic fields in the vicinity of the spectrometer. Also, magnetic fields may affect the low-energy electrons. These disturbing effects are likely to produce losses of the electron intensity at the low-energy limit. It is recalled that our auxiliary measurements with the gas target yielded reliable results at energies as low as 2 eV. During the experiment with the solid target, however, it was found that the intensity of electrons of energies less than 10 eV is less reproducible than those measured at higher energies. We estimated for the data with energies less than 10 eV an error of $\pm 50\%$. Hence we would not exclude that the solid target or the target holder produced spurious effects due to charge up.

The energy spectra of electrons emitted during the interaction of ions with solids exhibit a maximum at low energies. This maximum is influenced by refraction effects due to the potential step at the surface that produces a decrease of the electron intensity at small energies [35]. It should be noted that disturbing effects might shift the maximum in the electron spectrum to higher energies. In Fig. 1 the measured spectra exhibit a maximum at an energy about 5–7 eV. Similar results for the maxima in the energy spectra were previously obtained in measurements with highly charged ions [3,30]. For instance, the double differential yields by Zeijlmans van Emmichoven *et al.* [30] using highly charged N^{6+} ions show a maximum near an electron energy of 7 eV. The same was found by Delaunay *et al.* [3], who determined single differential electron yields. It is noted, however, that for light and singly charged ions a maximum of the electron distribution was observed at an energy of about 1–2 eV [36,37].

Since the absolute yields as well as the low-energy intensities may have significant uncertainties, it is useful to verify the reliability of the measured data. The double differential yields were integrated with respect to energy and angle to obtain total electron yields. It is noted that all total yields refer to the electrons ejected into the upper 2π-hemisphere. The integration is based on preliminary measurements of the angular dependence of the electron intensities. Since the observation angle is 40°, which is close to the magic angle, the total yield is rather insensitive to the angular distribution so that experimental uncertainties associated with the preliminary results of angular distribution are not important. The measured spectra exhibit a maximum at 5–7 eV. This maximum could be caused by disturbing effects, when the electron yield is spuriously suppressed at lower energies. To estimate the maximal error that can be produced by a spurious reduction of the low-energy electrons we performed an auxiliary calculation, assuming a constant double differential yield equal to the maximal value for the electrons with energies less than 10 eV. In this case the total electron yield increases by less than 20%. In Fig. 2 and Table I the present results are compared with measurements from Eder *et al.* [29], who claim a relatively high accuracy of about 4%. Those data show a constant yield γ of about 4.9 e^-/ion for N^{6+} projectile velocities up to 0.1 a.u., i.e., a projectile energy of about 5 keV. Above this energy the total electron yield starts to increase with increasing projectile velocity.

From Fig. 2 and Table I it is seen that the measured data and the values from Eder *et al.* [29] agree within the error bars. Thus the comparison provides confidence for the measured data so that a meaningful comparison can be made by means of the following model calculations.

III. COMPARISON WITH MODEL CALCULATIONS

The model used for the present simulation of the ion-induced electron emission is based on the classical over-the-barrier model by Burgdörfer *et al.* [7]. The model includes

TABLE I. Total yields for electron emission by N^{6+} incident on a monocrystalline Au surface for four different projectile energies. Total yields, obtained from integration of the measured results, are shown in comparison with corresponding yields by Eder *et al.* [29]. Also shown are total autoionization yields above the surface obtained by integration of the calculated spectra.

Projectile energy (keV)	Projectile velocity (a.u.)	Total yield γ measured (e^-/ion)	Total yield γ by Eder *et al.* (e^-/ion)	Autoionization yield above the surface (e^-/ion)
0.09	0.016	4.3 ± 1.7	4.9	4.9
0.27	0.028	5.5 ± 1.8	4.9	3.1
3	0.1	6.0 ± 1.5	4.9	1.1
60	0.4	7.2 ± 1.8	8.1	0.3

all processes above the surface such as image charge acceleration, resonant capture, resonant ionization, autoionization, and peel off. The above-surface processes have been linked via a system of coupled rate equations for the populations of hydrogenlike shells for the incoming projectile. Apart from the rate for autoionization, which is obtained from a semiempirical formula [7] based on the COWAN code [38], all other rates have been estimated on the basis of the classical over-the-barrier model.

These rates were applied in the Monte Carlo code by Lemell and collaborators [10,39] simulating the energy distribution of the emitted electrons due to autoionization and to compute the number distributions of the electron-emission processes. The approach towards the surface is modeled as a stepwise process with time intervals of about 0.1 a.u. The input parameters are the initial velocity, the incident angle, and the charge state of the particle as well as the characteristics of the solid. For each time interval the program determines the image charge acceleration, which, in turn, is used to calculate changes in the velocity and the direction of the particle. When the ion has reached the critical distance for electron capture, electrons are transferred from the solid to the projectile. From this starting point all other mechanisms become possible such as resonant ionization and autoionization. For this purpose probabilities were calculated for a process to take place within the time Δt using $P(t)=1-\exp(-R\Delta t)$, with R being the rate from Ref. [7]. Each process occurs as a random event determined by the Monte Carlo technique. When the ion finally enters the jellium edge weakly bound electrons are peeled off. Surprisingly, it turned out that the results of this program were quite insensitive to changes of the respective rates for resonant capture and loss of electrons from and to the conduction band.

Kurz *et al.* [10] applied the Monte Carlo simulation to calculate the total electron yield and electron-number distribution for highly charged ions incident on a clean gold surface. Their treatment involved only an estimate for energy- and direction-dependent probabilities for an electron to reach the detector. In this case the simulation led to a satisfactorily quantitative agreement with their experimental results. However, these calculation referred to the total yield and electron-number distribution and not to differential energy spectra of the emitted electrons. Raw electron energy spectra resulting from the model described above have been treated with refined escape fractions calculated according to [40] to make them comparable to experimental data without any further scaling. The applicability of the program to electron spectra above the surface has not been verified yet.

Figure 1 displays the results of the model calculations in comparison with the experimental data. It is important to recall that the model calculations refer to only autoionization processes above surface. The calculation treats an ensemble of typically 10^4 particles and therefore the results exhibit fluctuations due to limited statistics. In addition, it should be stated that the multiparticle nature of the problem, its semiclassical treatment, and other approximations may cause uncertainties in the result of the simulation.

Figure 1(a) refers to N^{6+} ions incident on Au with an energy of 90 eV corresponding to a velocity of 1.6×10^{-2} a.u. (Table I). The measured electron spectra exhibit only weak structures; note, for instance, the L Auger maximum at about 55 eV. In order to verify whether the structures are lost because of low resolution, the same measurements were made with high resolution, resulting in the same smooth spectra. In contrast, the corresponding theoretical spectra exhibit significant structures, which can be associated with the fact that the energies for the electrons bound to projectile are determined according to an atomic model neglecting part of the solid-state effects. In the Monte Carlo code the energies of these electrons were calculated without considering the energy shift due to the image charge and the outer screening. These effects would lead to a redistribution of the calculated emitted electrons resulting in a smoothing of the electron spectrum. We would not expect that this smoothing significantly affects the integrated yield of autoionization electrons.

In the case of 90 eV impact the double differential emission yield from the experiment and the calculation show surprisingly good agreement for low electron energies. The integrated yield of the simulated spectrum of 4.9 e^-/ion agrees with the measured total yield of 4.3 ± 1.7 e^-/ion; refer to Table I. For this projectile energy we can conclude that a major part of the ejected electrons originate from autoionization processes above surface.

Figure 1(b) refers to a projectile energy of 270 eV. In the low-energy region of the spectrum the measured double differential yields are about a factor 2 higher than the calculated yield for autoionization. Accordingly, the same value is found for the ratio between the measured total electron yields and the integrated calculated electron spectrum due to autoionization above surface (Table I). Hence, at a projectile energy of 270 eV approximately half of the electrons are emitted by autoionization above the surface.

Figures 1(c) and 1(d) demonstrate the behavior at higher projectile energies. Figure 1(c) displays the comparison between the calculated and experimental spectra at the projectile energy of 3 keV. Referring to Table I, the measured total yield is about a factor 5 higher than the corresponding result of the calculation. In the case of the highest projectile energy of 60 keV the measured double differential electron yield is more than a factor 10 higher than the simulated result; see Table I. This clearly shows that autoionization processes above the surface become negligible at high projectile velocities.

Therefore, at high impact energies the electron emission yield is dominated by processes other than above-surface autoionization. As discussed in the Introduction, different mechanisms, apart from autoionization, contribute to the electron emission of a highly charged ion interacting with a solid: (i) removal of previously captured electrons by level shifting, (ii) electron peel off at the surface, (iii) Auger processes filling low-lying orbitals of the hollow atom, and (iv) binary projectile-electron collisions in the solid. The intensities of below-surface electrons are enhanced by the production of secondary electrons.

The present Monte Carlo program provides also information about the number of electrons released above the surface due to energy level shifting caused by the image charge and screening effects. This number increases from 0.3 to 1.4 e^-/ion within the studied energy range. The number of electrons that are peeled off during the passage into the electron density of the surface amounts to a value of about 1 e^-/ion for all energies considered. These numbers show that the above-surface contributions are not sufficiently high to explain the observed low-energy electron intensities for fast projectiles.

Hence the below-surface mechanisms (iii) and (iv) become more important at higher projectile velocities. We expect the production of low-energy electrons via cascades of secondary electrons initiated by L and K Auger electrons ejected within the solid. Hughes *et al.* examined the total electron emission yield for projectile energies above 30 keV N^{q+} $(q=2,5,6)$ on Au [28]. In that work the secondary-electron-emission processes initiated by Auger transitions occurring within the target bulk are considered to be responsible for the difference in the total electron-emission yield between N^{5+} and N^{6+}. Moreover, for sufficiently fast projectiles we expect an increasing number of excited electrons inside the solid due to binary ion-electron collisions.

The present method of comparing theory with experiment also allows for the examination of the final step of the cascade filling the K shell. Figure 3 displays the comparison of the measured spectra with the model results in the energy range of the KLL Auger electron energy of N. Data are shown for the lower projectile energies of 90 and 270 eV. We note that for 3 keV and 60 keV the calculated yields for autoionization are found to be negligibly small.

For 90 eV projectiles the calculation predicts that about 10% of the KLL Auger electrons are emitted before the projectile reaches the surface. This number is consistent with the spectral fraction attributed to above-surface K Auger emission of N^{6+} on Ni by Das and Margenstern [41]. The 10% fraction corresponds to the total KLL Auger electron yield of 0.05 e^-/ion ejected into the upper 2π-hemisphere. The calculated value should be seen in relation to the measured yield for KLL Auger electrons, which amounts to 0.25 e^-/ion.

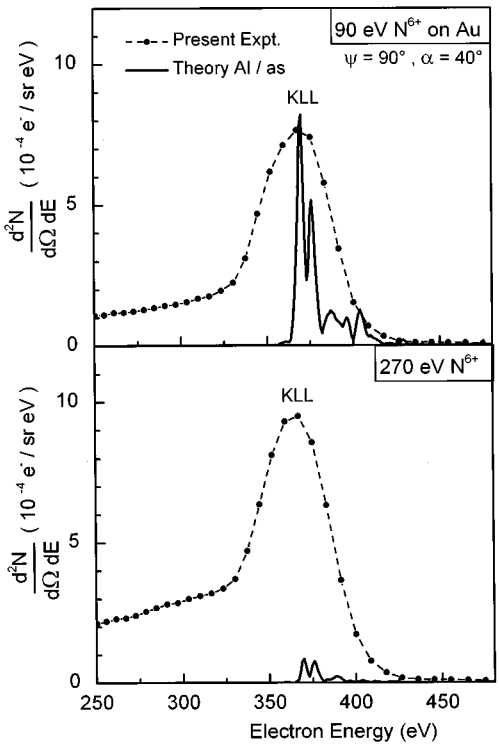

FIG. 3. Comparison of measured double differential cross sections (dots) in the energy range of the KLL Auger lines with model calculations (line) for N^{6+} incident on a Au surface for two different projectile energies like in Fig. 1. The simulation concerns merely the emitted electrons due to autoionization above the surface (AI/as).

For the projectile energy of 270 eV, the model predicts a fraction of about 1% of all atoms emitting the KLL Auger electron before hitting the surface. This number is equivalent to a total yield of 0.005 e^-/ion, which should be seen in connection with the measured KLL yield of 0.4 e^-/ion. The comparison of the measured data with the model results indicates that already at 270 eV nearly all K Auger transitions take place inside the solid.

IV. SUMMARY

In this work we study the formation and filling of hollow atoms in front of a surface by analyzing the ejection of low-energy electrons emitted from a metal surface. We measured the double different electron yields for different projectile energies from 90 eV to 60 keV of N^{6+} incident on Au. The comparison of the measured total yields with experimental results from Eder *et al.* [29] shows that our measurements reproduce these total electron yields within the error bars.

The measured electron spectra exhibit a maximum within the energy range 5–7 eV, which is consistent with previous measurements using highly charged ions [3,30]. However, measurements with singly charged ions exhibit a maximum at 2 eV [36]. Further studies are needed to elucidate the difference in the maximum values.

The experimental spectra were compared with results of a

Monte Carlo simulation based on the classical over-the-barrier model by Burgdörfer *et al.* [7]. For small projectile energies the Monte Carlo simulation of the low-energy electron spectrum shows good agreement with the measurement. It is an important conclusion of the present study that for slow projectiles of 90 eV the observed low-energy electrons can essentially be accounted for by above-surface autoionization considered previously by Arifov *et al.* [2]. It is noted, however, that uncertainties of the model calculation require some care with final conclusions.

The relaxation process by autoionization is limited by the interaction time in front of the surface. For slow projectiles of 90 eV the interaction time above the surface is comparatively long and therefore significant relaxation of the hollow atom can occur until the projectile hits the surface. Nevertheless, the deexcitation of the hollow atom caused by dielectronic processes is incomplete in front of the surface, i.e., the Auger transitions barely reach the K shell. The comparison of the measured electron yield with the calculation for autoionization above surface demonstrates that for 90 eV projectiles only a fraction of 10% relax in front of the surface including the final step of KLL Auger transitions.

The interaction time decreases with increasing projectile velocity. Thus, for projectile energies higher than 90 eV the final step of the Auger cascade occurs for practically all ions within the solid. The Auger electrons ejected below the surface may create an avalanche of secondary electrons that contribute to the low-energy part of the spectrum. Moreover, for fast projectiles the emission of low-energy electron is expected to be dominated by binary ion-electron collisions in the solid.

In the future we plan to examine the angular dependence of the emitted electrons further. Moreover, the contribution of secondary electrons released by Auger electrons below the surface shall be studied.

ACKNOWLEDGMENTS

We are indebted to Joachim Burgdörfer and Max Rösler for fruitful discussions. We acknowledge the support by the Human Capital and Mobility program under Contract No. CHRT-CT93-0103.

[1] H. D. Hagstrum, Phys. Rev. **96**, 325 (1954).
[2] U. A. Arifov, E. S. Mukhamadiev, E. S. Parilis, and A. S. Pasyuk, Zh. Tekh. Fiz. **43**, 375 (1973) [Sov. Phys. Tech. Phys. **18**, 240 (1973)].
[3] M. Delaunay, M. Fehringer, R. Geller, P. Varga, and H. P. Winter, Europhys. Lett. **4**, 377 (1987).
[4] S. T. De Zwart, Ph.D. thesis, Rijksuniversiteit Groningen, 1987 (unpublished).
[5] H. J. Andrä, Nucl. Instrum. Methods Phys. Res. B **43**, 306 (1989).
[6] J. P. Briand, L. De Billy, P. Charles, S. Essabaa, P. Briand, R. Geller, J. P. Desclaux, S. Bliman, and C. Ristori, Phys. Rev. Lett. **65**, 159 (1990).
[7] J. Burgdörfer, P. Lerner, and F. W. Meyer, Phys. Rev. A **44**, 5674 (1991).
[8] R. Köhrbrück, K. Sommer, J. P. Biersack, J. Bleck-Neuhaus, S. Schippers, P. Roncin, D. Lecler, F. Fremont, and N. Stolterfoht, Phys. Rev. A **45**, 4653 (1992).
[9] J. Burgdörfer, *Review of Fundamental Processes and Applications of Atoms and Ions* (World Scientific, Singapore, 1993), p. 517.
[10] H. Kurz, F. Aumayr, C. Lemell, K. Töglhofer, and H. P. Winter, Phys. Rev. A **48**, 2192 (1993).
[11] J. Burgdörfer, C. Reinhold, and F. Meyer, Nucl. Instrum. Methods Phys. Res. B **98**, 415 (1995).
[12] A. Arnau, F. Aumayr, P. M. Echenique, M. Grether, W. Heiland, J. Limburg, R. Morgenstern, P. Roncin, S. Schippers, R. Schuch, N. Stolterfoht, P. Varga, T. J. M. Zouros, and H. P. Winter, Surf. Sci. Rep. **27**, 113 (1997).
[13] H. Winter, Phys. Rev. A **46**, R13 (1992).
[14] H. Winter, C. Auth, R. Schuch, and E. Beebe, Phys. Rev. Lett. **71**, 1939 (1993).
[15] F. Aumayr, H. Kurz, D. Schneider, M. A. Briere, J. W. McDonald, C. E. Cunningham, and H. P. Winter, Phys. Rev. Lett. **71**, 1943 (1993).
[16] J. Burgdörfer and F. Meyer, Phys. Rev. A **47**, R20 (1993).
[17] C. Lemell, H. P. Winter, F. Aumayr, J. Burgdörfer, and F. Meyer, Phys. Rev. A **53**, 880 (1996).
[18] F. Aumayr and H. P. Winter, Comments At. Mol. Phys. **29**, 275 (1994).
[19] A. Arnau, R. Köhrbrück, M. Grether, A. Spieler, and N. Stolterfoht, Phys. Rev. A **51**, R3399 (1995).
[20] N. Stolterfoht, D. Niemann, M. Grether, A. Spieler, A. Arnau, C. Lemell, F. Aumayr, and H. P. Winter, Nucl. Instrum. Methods Phys. Res. B **124**, 303 (1997).
[21] M. Rösler, in *Particle Induced Electron Emission I*, edited by G. Höhler, Springer Tracts in Modern Physics Vol. 122 (Springer-Verlag, Berlin, 1991).
[22] L. Folkerts and R. Morgenstern, Z. Phys. D **21**, S351 (1991).
[23] H. Limburg, S. Schippers, I. Hughes, R. Hoekstra, R. Morgenstern, S. Hustedt, N. Hatke, and W. Heiland, Phys. Rev. A **51**, 3873 (1995).
[24] M. Grether, A. Arnau, R. Köhrbrück, A. Spieler, and N. Stolterfoht, Nucl. Instrum. Methods Phys. Res. B **115**, 157 (1996).
[25] N. Stolterfoht, A. Arnau, M. Grether, R. Köhrbrück, A. Spieler, R. Page, A. Saal, J. Thomaschewski, and J. Bleck-Neuhaus, Phys. Rev. A **52**, 445 (1995).
[26] M. Delaunay, M. Fehringer, R. Geller, D. Hitz, P. Varga, and H. P. Winter, Phys. Rev. B **35**, 4232 (1987).
[27] F. Aumayr, G. Lakits, and H. P. Winter, Appl. Surf. Sci. **47**, 139 (1991).
[28] I. G. Hughes, J. Burgdörfer, L. Folkerts, C. C. Havener, S. H. Overbury, M. T. Robinson, D. M. Zehner, P. A. Zeijlmans van Emmichoven, and F. W. Meyer, Phys. Rev. Lett. **71**, 291 (1993).
[29] H. Eder, M. Vana, F. Aumayr, H. P. Winter, J. I. Juaristi, and A. Arnau, *Procedings of the Conference on the Physics of Highly Charged Ions, Saitama, 1996* [Phys. Scr. (to be published)].

[30] P. A. Zeijlmans van Emmichoven, C. C. Havener, and F. W. Meyer, Phys. Rev. A **43**, 1405 (1991).
[31] P. A. Zeijlmans van Emmichoven, C. C. Havener, I. G. Hughes, D. M. Zehner, and F. W. Meyer, Phys. Rev. A **47**, 3998 (1993).
[32] N. Stolterfoht, Z. Phys. **248**, 81 (1971).
[33] A. Spieler, Ph.D. thesis, Technische Universität Berlin, 1996 (unpublished).
[34] N. Stolterfoht, C. C. Havener, R. A. Phaneuf, J. K. Swenson, and S. M. Shafroth, Phys. Rev. Lett. **57**, 74 (1986).
[35] J. Thomaschewski, J. Bleck-Neuhaus, M. Grether, A. Spieler, D. Niemann, and N. Stolterfoht, Nucl. Instrum. Methods Phys. Res. B **125**, 163 (1997).
[36] D. Hasselkamp, in *Particle Induced Electron Emission II*, edited by G. Höhler, Springer Tracts in Modern Physics Vol. 123 (Springer-Verlag, Berlin, 1992).
[37] R. A. Baragiola and C. A. Dukes, Phys. Rev. Lett. **76**, 2547 (1996).
[38] R. D. Cowan, *The Theory of Atomic Structure and Spectra* (University of California Press, Berkeley, 1981).
[39] C. Lemell, Master's thesis, Technische Universität Wien, Austria, 1993 (unpublished).
[40] C. Lemell, H. P. Winter, F. Aumayr, J. Burgdörfer, and C. Reinhold, Nucl. Instrum. Methods Phys. Res. B **102**, 33 (1995).
[41] J. Das and R. Morgenstern, Phys. Rev. A **47**, R755 (1993).